PHYSICAL REVIEW B VOLUME 17, NUMBER 4 15 FEBRUARY 1978

Effects of interband excitations on Raman phonons in heavily doped *n*-Si

Meera Chandrasekhar,* J. B. Renucci,† and M. Cardona
Max-Planck-Institut für Festkörperforschung, 7000 Stuttgart-80, Federal Republic of Germany
(Received 13 October 1977)

Raman-active inter-conduction-band transitions from the Δ_1 to $\Delta_{2'}$ bands in heavily doped n-Si ($n \simeq 1.5 \times 10^{20}$ cm^{-3}) interfere with the zone-center optical phonon to produce Fano-type asymmetric phonon line shapes typical of a discrete-continuum interaction. We have studied the line shapes as a function of exciting frequency and uniaxial stress along the [001] and [111] directions. The asymmetry is removed under [001] uniaxial stress for the doublet component of the phonon that couples to the stress-depleted doublet valley, and is enhanced for the singlet component that couples to the carrier-enhanced singlet valley. We have calculated from microscopic theory the parameters that describe the Fano interaction—the asymmetry parameter, the broadening, and the frequency shift due to the self-energy of the phonon deformation-potential interaction with the free electrons in the conduction-band valley. These parameters have been calculated for zero stress and a high stress along the [001] direction, and are found to be in excellent agreement with experiment. We have also investigated the second-order acoustical-phonon scattering [2TA(X)]; it shows no change in line shape for heavily doped n-Si. Under uniaxial stress along the [001] and [111] directions, it exhibits only the hydrostatic shift, as does pure Si, which was measured for comparison.

I. INTRODUCTION

In heavily doped n-type Si ($n \simeq 1.5 \times 10^{20}$ cm^{-3}) the partial filling of the $\langle 001 \rangle$ conduction-band valleys makes possible transitions between the Δ_1 and $\Delta_{2'}$ conduction bands that are along the $\langle 100 \rangle$ directions. These transitions are infrared forbidden but Raman active. When the doping is sufficiently high, the energy continuum of these transitions overlaps with the energy of the discrete Raman-active optical phonon of the same symmetry and an interference between the phonon and the electronic transitions takes place.[1,2] The line shape of the phonon is modified to a typically asymmetric Fano-type line shape characteristic of a discrete-continuum interaction.[3] Similar effects have been observed in heavily doped p-type Si,[4] where inter-valence-band transitions are responsible for the interference with the optical phonon. In addition to the asymmetric line shape, a small shift in the position of the phonon to lower frequencies is observed. This frequency shift may be described as the real part of the self-energy due to the phonon deformation-potential interaction with the free electrons in the conduction band.[5]

We present in this paper experimental results and theoretical calculations in heavily doped n-Si for the parameters that describe the Fano-type asymmetry: the asymmetry parameter q, broadening Γ and the frequency shift $\Delta\omega_0$. Through a purely algebraic approach we calculate values of these parameters that are in good agreement with experiment. These calculations also yield the sign of the Fano asymmetry parameter q which, contrary to previous statements,[6] is not determined by symmetry. We have also measured the shifts in the frequency of the phonon for heavily doped Si as a function of uniaxial stress along the [001] direction. The changing valley populations cause changes in $\Delta\omega_0$, q, and Γ. The parameters are calculated for a high stress, and found to agree well with experiment. For a [111] uniaxial stress, the valley populations remain unchanged, and the three parameters do not change with stress.

The Fano line shape of the phonon is also studied as a function of the exciting frequency. In a region far from the E_1 resonance,[7] the contribution to the scattering due to the phonon varies as Ω^4 (Ω is the laser frequency) while the contribution from the inter-conduction-band excitations is nearly independent of frequency.[8] The asymmetry parameter q for several frequencies is determined experimentally and theoretically, and both values are found again to be in good agreement. Γ and $\Delta\omega_0$ are independent of exciting frequency.

The frequency of the second-order transverse-acoustical phonon 2TA(X) was also studied under uniaxial stress along the [001] and [111] crystal directions for both pure Si and heavily doped n-Si. The phonon is of nearly spherical (Γ_1) symmetry, so that only a hydrostatic shift is observed, with a coefficient in agreement with previous measurements. No change in the line shape, either due to the doping in the heavily doped material (the low-frequency tail due to intraband scattering[2] is weak in intensity at the frequency of this phonon), or under stress for either material, is observed.

 © 1978 The American Physical Society

II. EXPERIMENTAL DETAILS

Raman spectra were taken at room temperature in the backscattering configuration standard for opaque materials. Spectra Physics Ar^+ and Kr^+ lasers were used to obtain the exciting radiation. A Spex triple monochromator with a wavenumber drive and a cooled photomultiplier equipped with photon counting electronics was used for detection, in conjunction with a multichannel analyzer for data storage. Counting times of 2–5 sec per channel were utilized to record first-order spectra and 30 sec per channel for second-order spectra. The stress apparatus employed was equipped with a digital readout as has been described previously in the literature.[9] Typically, compressive stresses up to 20 kbar were reached. A neon lamp was used for wavelength reference and calibration purposes.

Samples of Si were cut from single crystals, and x-ray oriented to within 1°. The samples were cut into bars of $20 \times 1.3 \times 1.3$ mm, and the stress was applied along their length. The face used for scattering was polished with 0.3-μm alumina, polish etched with Syton[10] for 10 min and etched in HF for 1 min.

III. THEORY

The presence of electrons in the ⟨100⟩ conduction-band valleys permits infrared forbidden but Raman allowed transitions between the Δ_1 and $\Delta_{2'}$ conduction bands. A continuum of transitions exists from a minimum energy $\hbar\omega_{min}$ to a maximum energy $\hbar\omega_{max}$ [Fig. 1(a)] which are determined by the Fermi level E_F. If the energy of the discrete optical-phonon state, which has the same symmetry as the interband transitions, falls within the continuum, an interference between the discrete state and the continuum takes place. Such an interference has been treated by Fano[3] and is known to lead to asymmetric line shapes. Fano's theory has been adapted to the case of a quasicontinuum as in p- and n-type Si.[4,11] The asymmetric line shape of the phonon is given by

$$I(\epsilon, q) = (q+\epsilon)^2/(1+\epsilon^2) , \qquad (1a)$$

where

$$\epsilon = (\omega - \omega_0 - \Delta\omega_0)/\Gamma \qquad (1b)$$

and

$$q = (VT_p/T_e + \Delta\omega_0)/\Gamma , \qquad (1c)$$

where q is the asymmetry parameter and Γ the broadening. ω_0 is the phonon frequency in pure Si, and $\omega_0 + \Delta\omega_0$ the frequency in heavily doped Si. The three parameters q, Γ, and $\Delta\omega_0$ are related to the microscopic properties of the crystal. The parameter q, as defined in Eq. (1c), depends on Γ and $\Delta\omega_0$, the electron-phonon matrix element

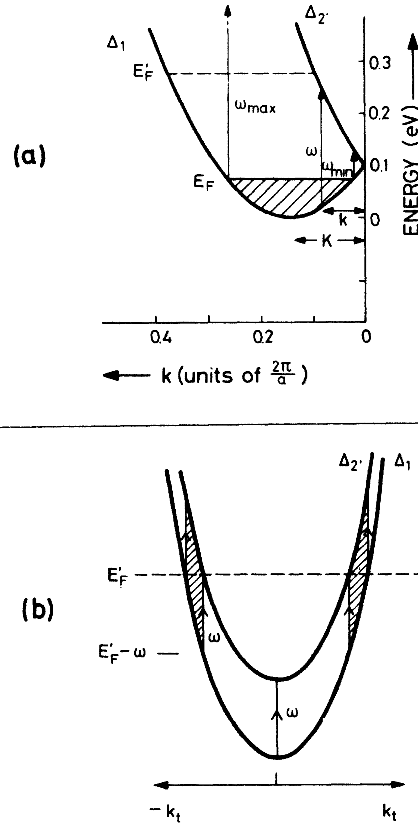

FIG. 1. (a) Conduction bands of Si near the X_1 point (where the Δ_1 and $\Delta_{2'}$ bands are degenerate). $\hbar\omega$ is the energy of a Raman-active transition between bottom of the conduction band and the edge of the Brillouin zone. $\hbar\omega_{min}$ and $\hbar\omega_{max}$ are the minimum and maximum transition energies between the Δ_1 and $\Delta_{2'}$ bands for the Fermi level of E_F. E_F' denotes the Fermi level when it has risen above the X_1 point. (b) Transverse slice of the bands at an energy $\hbar\omega < \hbar\omega_{min}$ when the Fermi level has risen above the X_1 point to E_F'. The shaded area denotes the region where there exist filled initial and empty final states, permitting transitions to take place.

V, and the Raman matrix elements between the ground and excited states of the phonon and electron, T_p and T_e, respectively. The broadening Γ and the frequency shift $\Delta\omega_0$ (which is the real part of the self-energy due to interaction with free electrons in the conduction band) are given by

$$\Gamma = \pi V^2 D(\omega), \qquad (2a)$$

$$\Delta\omega_0 = V^2 R(\omega) , \qquad (2b)$$

where

$$R(\omega) = \mathrm{P} \int D(\omega')\left(\frac{1}{\omega - \omega'} + \frac{1}{-\omega - \omega'}\right) d\omega' . \qquad (2c)$$

P represents the principal value of the integral, while $D(\omega)$ is the combined density of states for the electronic transitions, a function of the transition energy $\hbar\omega$.

In n-type Si, the parameters $\Delta\omega_0$, q, and Γ can be calculated algebraically from microscopic theory if we assume that the conduction bands Δ_1 and $\Delta_{2'}$ are parabolic. This assumption is reasonable in view of previous calculations[12,13] and experiments.[14] The transverse and longitudinal masses of the bands m_t and m_l are known from experiment,[14] as is the distance of the minimum of the Δ_1 conduction band from the edge of the Brillouin zone[12] at X_1, $K=(2\pi/a)\times 0.14$, where a is the lattice constant [Fig. 1(a)]. We proceed to evaluate from microscopic theory the parameters q, Γ, and $\Delta\omega_0$.

A. Calculation of $\Delta\omega_0$

The density of states per unit volume, $D(\omega)$ is given by the standard expression[15]

$$D(\omega)=\frac{1}{4\pi^3}\int\frac{dS_\omega}{\nabla_{\vec{k}}(\hbar\omega)}\ , \tag{3}$$

where dS_ω is the element of area in k space of the surface of constant energy $\hbar\omega$. Assuming that the Δ_1 and $\Delta_{2'}$ bands have equal masses, the transition energy between the two bands, $\hbar\omega$, at a wave vector whose longitudinal component is k, is given by [Fig. 1(a)]

$$\begin{aligned}\hbar\omega &= (\hbar^2/2m_l)[(K+k)^2-(K-k)^2]\\ &=(\hbar^2/2m_l)4Kk\ .\end{aligned} \tag{4}$$

Therefore,

$$\nabla_{\vec{k}}(\hbar\omega)=2K\hbar^2/m_l\ , \tag{5}$$

since the transverse contribution is zero. dS_ω is the transverse slice of the mass ellipsoid at energy $\hbar\omega$, which in terms of the transverse component of the wave vector k_t is given by

$$dS_\omega=\pi k_t^2\ . \tag{6}$$

When E_F is at or below the X_1 point, where the Δ_1 and $\Delta_{2'}$ bands are degenerate, as in Fig. 1(a), the energy in the transverse direction, proportional to k_t^2, is written as the difference between the Fermi energy E_F and the energy along the longitudinal direction of the Δ_1 band. At a point where the longitudinal component of the wave vector is k,

$$\hbar^2k_t^2/2m_t=E_F-(\hbar^2/2m_l)(K-k)^2 \tag{7a}$$

$$=E_F-(\hbar^2/2m_l)(K-\omega m_l/2K\hbar)^2\ . \tag{7b}$$

The density of states per unit volume $D(\omega)$ is found by substituting Eqs. (5)–(7) into Eq. (3),

$$D(\omega)=\frac{1}{4\pi^2}\frac{m_lm_t}{K\hbar^4}\left[E_F-\frac{\hbar^2}{2m_l}\left(K-\frac{\omega m_l}{2K\hbar}\right)^2\right]. \tag{8}$$

The electron-phonon matrix element for the deformation potential interaction is[16]

$$V=(2/a)D_0(\hbar/4MN\omega_0)^{1/2}\ , \tag{9}$$

where M is the atomic mass of Si, $N=4/a^3$ is the number of unit cells per unit volume and D_0 is the phonon deformation potential at the [100] conduction bands in Si. There are no known measurements of this quantity, and a calculated value of -8.08 eV is assumed[17] (see Appendix A). We use[15] $a=5.43$ Å and[14] $m_l=0.9163\ m_e$, $m_t=0.1905\ m_e$, where m_e is the electronic mass.

The expression (2b) for $\Delta\omega_0$ is obtained from standard perturbation theory as the real part of the self-energy of the phonon due to interaction with the free electrons.[5] It represents the anharmonic contribution to the frequency of the phonon. The expression for the frequency shift is obtained at the phonon frequency ω_0, using $R(\omega_0)$ from Eq. (2c) and substituting Eq. (9) into Eqs. (2b) and (2c),

$$\Delta\omega_0=2\frac{D_0^2}{a^2}\frac{\hbar}{MN\omega_0}\times \mathrm{P}\int_{\omega_{\min}}^{\omega_{\max}}D(\omega')\left(\frac{1}{\omega_0-\omega'}+\frac{1}{-\omega_0-\omega'}\right)d\omega'\ . \tag{10}$$

The factor of 2 accounts for the fact that a [001] phonon interacts with the two equivalent [001] and [00$\bar{1}$] valleys. The limits of integration $\omega_{\max}$ and $\omega_{\min}$ are easily calculated using the Fermi level and the band parameters. Substituting Eq. (8) into Eq. (10) and performing the rather straightforward integration, we obtain $\Delta\omega_0$ in closed form

$$\begin{aligned}\Delta\omega_0=\frac{D_0^2am_lm_t}{8M\omega_0\pi^2\hbar^4K}\Bigg[&\left(\frac{m_l}{8K^2}(\omega_{\max}^2-\omega_{\min}^2)-\hbar(\omega_{\max}-\omega_{\min})\right)+\left(\frac{m_l}{8K^2}\omega_0^2-\frac{\hbar\omega_0}{2}-E_F+\frac{\hbar^2K^2}{2m_l}\right)\ln\left|\frac{\omega_0-\omega_{\max}}{\omega_0-\omega_{\min}}\right|\\ &+\left(\frac{m_l}{8K^2}\omega_0^2+\frac{\hbar\omega_0}{2}-E_F+\frac{\hbar^2K^2}{2m_l}\right)\ln\left|\frac{\omega_0+\omega_{\max}}{\omega_0+\omega_{\min}}\right|\Bigg]\ .\end{aligned} \tag{10a}$$

Upon the application of a uniaxial stress along the [001] direction, the changes in the valley populations for the carrier enhanced singlet and the depleted doublet (Sec. IV B) are reflected in the Fermi level E_F and a consequent change in the limits of integration ω_{max} and ω_{min}. ω_{max} increases continuously with increasing E_F. ω_{min} decreases to zero up to the point when the Fermi level reaches the X_1 point for $E_F = 0.11$ eV. After that ω_{min} increases since the final states in the $\Delta_{2'}$ band begin to fill up. No transitions of energies between zero and $\hbar\omega_{min}$ are possible at $k_t = 0$. However, occupied initial and empty final states are available at larger values of k_t in the transverse direction. A transverse slice of the Δ_1 and $\Delta_{2'}$ bands is depicted in Fig. 1(b), for a transition energy $0 \leq \hbar\omega \leq \hbar\omega_{min}$, when the Fermi energy is above the X_1 point, e.g., at E_F'. Since the Δ_1 and $\Delta_{2'}$ conduction bands have equal masses, the energy separation between them $\hbar\omega$ remains constant for the transverse slice, defined by the value of the longitudinal component of the wavevector k [Fig. 1(b)]. Transitions occur only between the filled initial and empty final states, indicated by the shaded area for a Fermi level E_F'. In such a case, the transverse slice of the mass ellipsoid contributing to dS_ω will not be given by the circle implied in Eq. (6) but by the difference of two circles, one representing the empty $\Delta_{2'}$ band, the other the filled Δ_1 band. If we consider a transition whose final state is at energy E_F' in Fig. 1(b), the k_t's of these circles are defined by

$$(\hbar^2/2m_t)k_{t,max}^2 = E_F' ,$$
$$(\hbar^2/2m_t)k_{t,min}^2 = E_F' - \hbar\omega . \tag{11}$$

By subtracting the areas of the two circles in Eq. (11), we obtain an area [to replace that of the circle of radius k_t in Eq. (6)] which is independent of the Fermi level E_F',

$$dS_\omega' = \pi k_{t,max}^2 - \pi k_{t,min}^2 = 2\pi(m_t/\hbar)\omega . \tag{12}$$

This expression applies for the entire shaded area in Fig. 1(b). The density of states in this region is then obtained by substituting Eqs. (12) and (5) into Eq. (3):

$$D'(\omega) = (1/4\pi^2)(m_l m_t/K\hbar^3)\omega . \tag{13}$$

The contribution to $\Delta\omega_0$ from the filled region is, therefore,

$$\Delta'\omega_0 = \frac{1}{2\pi^2}\frac{D_0^2}{a^2}\frac{1}{MN\omega_0}\frac{m_l m_t}{K\hbar^2} \times \int_0^{\omega_{min}} d\omega\left(\frac{\omega}{\omega_0-\omega} + \frac{\omega}{-\omega_0-\omega}\right), \tag{14}$$

in analogy with Eq. (10). Upon integration, we obtain

$$\Delta'\omega_0 = \frac{D_0^2 a m_l m_t}{8M\omega_0\pi^2\hbar^3 K}\left(-2\omega_{min} + \omega_0 \ln\left|\frac{\omega_{min}+\omega_0}{\omega_{min}-\omega_0}\right|\right). \tag{14a}$$

This contribution is added to $\Delta\omega_0$ obtained from Eq. (10a) when the Fermi level rises above the X_1 point.

For the sample under study the Fermi energy at zero stress is 0.11 eV (as calculated using the method in Ref. 18), so that we start with the Fermi level at the X_1 point and $\omega_{min} = 0$ obtaining a contribution to $\Delta\omega_0$ only from Eq. (10a). On the application of a compressive uniaxial stress along the [001] direction, the singlet gains carriers, so that E_F rises above the X_1 point. At a high stress, the contribution due to the filled part, Eq. (14a) has to be considered, and is found, for $E_F = 0.22$ eV (corresponding to a stress of 20 kbar in our case) to be approximately equal to half of the contribution from Eq. (10a). The doublet at high stress is depleted of carriers and the contribution to $\Delta\omega_0$ comes only from Eq. (10a) with the appropriate ω_{max} and ω_{min}.

B. Calculation of Γ and q

The expression for the broadening Γ is given by Eq. (2a). The largest contribution from the density of states to the broadening is expected to be at the frequency of the phonon. We therefore calculate the broadening as

$$\Gamma = 2\pi(\hbar/MN\omega_0)(D_0^2/a^2)D(\omega_0) , \tag{15}$$

substituting Eq. (9) into Eq. (2a). $D(\omega_0)$ is obtained from Eq. (8). Once again the factor of 2 accounts for the fact that each phonon interacts with two equivalent valleys.

At zero stress, when the Fermi level is below the X_1 point, the calculation of $D(\omega_0)$ proceeds according to Eqs. (3)–(7), substituting ω_0 for ω, the condition being that the right-hand side in Eq. (7b) can only be positive. A negative value for k_t^2 indicates that the Fermi energy is lower than the initial state of the transition energy, in this case $\hbar\omega_0$. The electronic continuum does not then overlap with the phonon, and no contribution to Γ can occur due to the Fano interaction, i.e., $\Gamma = 0$. Such a case occurs for the doublet at a high stress along the [001] direction (Sec. IV B).

As the Fermi level rises well above the X_1 point filling states in the $\Delta_{2'}$ band beyond the energy $\hbar\omega = \hbar\omega_0$, as in the case of the singlet valley at 20 kbar, k_t at $\omega = \omega_0$ corresponds to $\hbar^2 k_t^2/2m_t = \hbar\omega_0$. This is the maximum possible value of k_t, regardless of how much higher the Fermi level

rises. This value of k_t was used to calculate Γ for the singlet at 20 kbar.

The asymmetry parameter q is defined in Eq. (1c). The Raman matrix element for the phonon T_p is obtained using the calculated value of the Raman tensor[19] $\mathcal{P}$ at the exciting frequency Ω,

$$T_p = \mathcal{P}[(\hbar/4MN\omega_0)(n_B+1)]^{1/2}(8\Omega^2/a^3) , \tag{16}$$

where n_B is the Bose-Einstein factor. The electronic matrix element is calculated using the valence band at X_4 as an intermediate state. The energy difference between the valence and conduction bands, $E_c - E_v$, is taken to be 4.4 eV. Then,[20]

$$T_e = \frac{e^2}{m^2}\sum_v (\langle\Delta_{2'}|p_x|v\rangle\langle v|p_y|\Delta_1\rangle + \langle\Delta_{2'}|p_y|v\rangle\langle v|p_x|\Delta_1\rangle) \times\left(\frac{1}{\hbar\Omega-(E_v-E_c)} - \frac{1}{\hbar\Omega+(E_v-E_c)}\right). \tag{17}$$

The summation runs over the wave functions of the valence band, denoted by v. The transition matrix elements are found using pseudopotential calculations (see Appendix A).

Using Eqs. (16) and (17) for T_p and T_e, Eq. (9) for V, Eq. (10) for $\Delta\omega_0$, and Eq. (15) for Γ, we substitute in Eq. (1c) to obtain the value of q. We note that Γ is independent of exciting frequency Ω, as are V and $\Delta\omega_0$, but the Raman matrix elements T_p and T_e are dependent on Ω, and the asymmetry defined by q is thus dependent on exciting frequency.

When a uniaxial stress along the [001] direction is applied, changes in Γ and $\Delta\omega_0$ due to changes in the Fermi level are reflected in q (Sec. IV B). The other parameters V, T_p, and T_e do not depend on the Fermi level.

Unlike the case of p-type Si,[4] the interference in n-type Si is small, so that the broadening due to the Fano interaction is small compared to the natural linewidth of pure Si. In order to get the correct line shape, the Fano line shape [Eq. (1a)] is convoluted with a Lorentzian corresponding to pure Si. The convoluted line shape is also Fano-like, with the form

$$I(q,\epsilon') = \frac{\Gamma}{\Gamma+\gamma}\,\frac{(q+\epsilon')^2}{1+\epsilon'^2} + \frac{\gamma}{\Gamma+\gamma} , \tag{18a}$$

where

$$\epsilon' = (\omega - \omega_0 - \Delta\omega_0)/(\Gamma+\gamma) \tag{18b}$$

and γ is the linewidth of the phonon in pure Si. Equation (18a) has the same form as Eq. (1a) except for a constant amplitude factor that corresponds to normalizing the intensities between the Lorentzian and the convoluted line shape of Eq. (18a) and a background $\gamma/\Gamma+\gamma$ which ensures that Eq. (18a) and Eq. (1a) have the same limit for $\omega\to\pm\infty$. The new line shape has the same q as Eq. (1a), but the broadening is the sum of the intrinsic broadening and the Fano interaction induced component. In comparing theory and experiment, one has to account for the natural linewidth of the phonon.

IV. RESULTS AND DISCUSSION

A. Zone-center phonon in the absence of stress

The one-phonon Raman spectrum for n-Si ($n = 1.5\times10^{20}$ cm^{-3}) was measured at room temperature for several exciting frequencies (Fig. 2). The experimental line shapes were fitted with the theoretical expression given by Eq. (18a), using the broadening $\Gamma+\gamma$, the asymmetry parameter q and the phonon frequency $\omega_0+\Delta\omega_0$ as adjustable parameters. Good fits were obtained in all cases.

Upon varying the exciting frequency Ω, no change is seen in Γ and $\Delta\omega_0$ within experimental error. This is consistent with the theoretical formulation of Sec. III. The only change is in the asymmetry parameter q, which increases, decreasing the asymmetry, as Ω increases. Physically, this arises mainly from the fact that the scattering due to interband transitions that exist from nearly zero frequency are almost independent of exciting frequency[8] while the phonon exhibits an Ω^4 behavior at energies far from the energy gap[7] (in this case

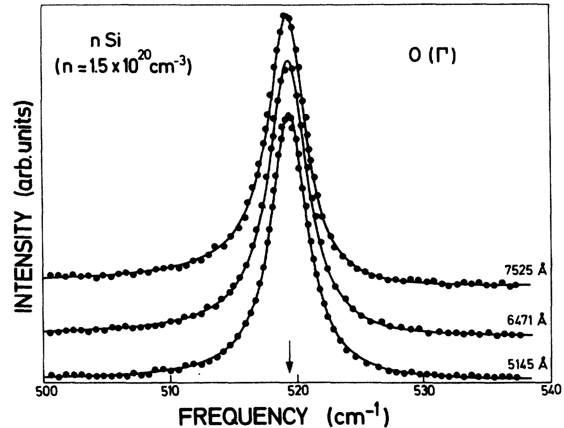

FIG. 2. Line shape of the zone-center optical phonon in heavily doped n-Si ($n\simeq1.5\times10^{20}$ cm^{-3}) as a function of exciting frequency. Note the decrease in the asymmetry of the line shape at 5145 Å as compared to 7525 Å. The intensities have been adjusted to be roughly equal. The dots are experimental points and the solid lines fits to Eq. (18a) using the values of q quoted in Table I. The average value of $\gamma+\Gamma$ obtained from these fits is 1.87 ± 0.1 cm^{-1}.

the degenerate E_0' and E_1 gaps at 3.4 eV).

Using the calculated values of Γ and $\Delta\omega_0$ ($\Gamma = 0.14 \pm 0.04$ cm^{-1}, $\Delta\omega_0 = -0.65$ cm^{-1}), which we shall discuss shortly, we calculate q according to the formulas of Sec. III. We notice first that the sign of q is determined by the numerator of Eq. (1c), since Γ is positive. The electron-phonon matrix element V is *negative* for the wave functions we have used to calculate D_0 [see Appendix A, Eqs. (A7) and (A8)]. The same wave functions are used to calculate the electronic matrix element T_e, which is also *negative* [Eq. (A11)] below the E_2 gap of 4.4 eV. Our measurements span the range from 1.65 to 2.4 eV. The phonon matrix element T_p is dependent on the sign of the Raman tensor $\mathcal{P}$, which has been determined to be negative from Fano interference line shapes in p-type Si.[20] Therefore, since both terms VT_p/T_e and $\Delta\omega_0$ are negative, the sign of q is negative, which means that the antiresonance in the line shape should be on the high-frequency side, as borne out by experiment. This case is opposite to that of p-type Si,[4] where the antiresonance is on the low-frequency side because of a positive q. It should be noted that the sign of q is not a consequence of symmetry as has been previously claimed[6] but of the signs of the matrix elements T_p, T_e, and V all of which do not follow simply from symmetry.

In Table I we list experimental and theoretical values of q for several exciting frequencies. Within experimental error excellent agreement is found. Values of $\mathcal{P}(\Omega)$ are obtained from Ref. 19

The frequency shift $\Delta\omega_0$ as calculated according to Eq. (10a) (at a zero stress Fermi level of 0.11 eV) is $\Delta\omega_0 = -0.65$ cm^{-1}, in excellent agreement with the experimental value of -0.5 ± 0.2 cm^{-1}. Using a semiclassical treatment for the electron-phonon interaction between the Δ_1 and $\Delta_{2'}$ bands, Cerdeira[17] obtained an approximate expression for $\Delta\omega_0$ as a function of the average transition energy $E_G(0)$,

TABLE I. Experimental and calculated values of the asymmetry parameter q for several exciting wavelengths.

Exciting wavelength (Å)	q (expt.)	q (theor.)
5145	-50 ± 10	-46^{+18}_{-10}
6471	-24 ± 2	-21^{+8}_{-4}
6764	-20 ± 2	-16^{+6}_{-4}
7525	-13 ± 1	-12^{+5}_{-3}

$$\Delta\omega_0 = -[D_0^2 a N_d / 6M\omega_0 E_G(0)][1 + E_F/E_G(0)] , \quad (19a)$$

where N_d is the carrier concentration. The leading term in this expression is obtained simply from Eq. (10) by substituting the number of carriers per valley $N_d/6$ for the integrated density of states $D(\omega)$ and an average transition energy $E_G(0)$ for ω', thereby dropping the integral. In the limit $\omega' = E_G(0) \gg \omega_0$,

$$\Delta\omega_0 = -(D_0^2 a/M\omega_0)(N_d/6)[1/E_G(0)] \quad (19b)$$

after replacing N by $4/a^3$. Equation (19a) yields results in good agreement with our detailed calculations if one uses for $E_G(0)$ 0.4 eV, a value which is reasonable in view of the limits of integration in Eq. (10) at zero stress.

The broadening Γ is calculated with Eq. (15) to be 0.14 ± 0.04 cm^{-1} (assuming an uncertainty of 10% in the Fermi level), while the experimental value obtained by subtracting an intrinsic broadening (that which corresponds to pure Si) of $\gamma = 1.55 \pm 0.1$ cm^{-1} from the linewidth of the phonon in the heavily doped Si is $\Gamma = 0.32 \pm 0.14$ cm^{-1}. However, if one assumes that the intrinsic linewidth is not that of pure Si but that of the carrier depleted doublet under a high uniaxial stress along a [001] direction, $\gamma = 1.76 \pm 0.14$ cm^{-1}, one obtains $\Gamma = 0.11 \pm 0.14$ cm^{-1} for our heavily doped crystal. This assumption would mean that there is a contribution to the linewidth of 0.2 cm^{-1} due to the disorder introduced by the dopant (different atomic masses, different force constants). The effect of the mass difference between the dopant phosphorous and silicon ($\Delta M/M = \frac{1}{15}$) is expected to be

$$\Delta\omega/\omega \simeq \tfrac{1}{2}(\Delta M/M)\, N_P/N_{Si} , \quad (20)$$

where N_P is the density of phosphorous and N_{Si} that of silicon atoms. If we assume that all phosphorous atoms are electrically active, N_P equals the electron concentration $N_d = 1.5 \times 10^{20}$ cm^{-3} in our case. Equation (20) then yields $\Delta\omega \simeq 0.05$ cm^{-1}. A contribution of the same order is expected from the changes in bond lengths around the phosphorous atoms. These contributions together explain qualitatively the disorder induced broadening of 0.2 cm^{-1} mentioned above.

In the light of the large relative errors in the experimental values of Γ, we do not consider the comparison between experimental and theoretical Γ's very meaningful. We believe that q and $\Delta\omega_0$ are more accurate indicators of the correctness of the calculations and the parameters used than Γ.

B. Zone-center phonon in the presence of stress

The one-phonon spectrum has been studied under the application of compressive uniaxial stresses

along the [001] and [111] crystal directions. In both cases the exciting radiation was 6471 Å. In order to compare the results obtained for heavily doped Si, the experiments were performed on pure Si under similar conditions. A neon calibration lamp was used in order to determine the frequencies of the phonon peaks to within 0.25 cm^{-1}.

Under the application of a uniaxial stress along the [001] direction, the three equivalent ⟨001⟩ conduction-band valleys (actually six in number, but since a uniaxial stress has even parity, only three need to be considered) split into a doublet [100] and [010] perpendicular to the stress and a singlet [001] parallel to the stress direction. For a compressive stress, as in the present case, the singlet is lower in energy than the doublet, consequently the carrier concentration and the Fermi level of the singlet valley are enhanced at the expense of the doublet valleys. The uniaxial stress also splits the triply degenerate zone-center optical phonon into a singlet Ω_s and a doublet Ω_d. The phonon singlet, which couples to the carrier enhanced singlet conduction band valley, experiences a stronger Fano interaction at a high stress, resulting in a phonon line shape with stronger asymmetry (lower q), larger broadening Γ, and a larger frequency shift due to the self-energy $\Delta\omega_0$. The phonon doublet Ω_d, however, couples to the carrier depleted doublet valleys, and has a more symmetric (higher q), narrower line shape, with a lowered $\Delta\omega_0$. The doublet at high stress, therefore, approaches the case of pure Si in line shape and frequency.

In Fig. 3 we plot the line shapes of the optical phonon at zero stress and at a high stress (20 kbar) along the [001] direction. The exciting radiation was 6471 Å. The spectrum obtained at zero stress is shown by the dots, while the solid line through the dots is the fit with Eq. (18a). At a stress of 20 kbar, we plot, for the sake of clarity, only the fits obtained for the phonon singlet and doublet Ω_s and Ω_d. The long dashes denote the singlet Ω_s that couples to the carrier enhanced singlet valley, and exhibits a stronger asymmetry and larger broadening, while the short dashes denote the doublet, narrower and more symmetric, approaching the line shape in pure Si. The singlet and doublet were separated by choosing appropriate polarizations: for a [001] stress axis, the doublet is observed for incident light polarized parallel and scattered light perpendicular to the stress axis (∥,⊥), and the singlet for a (⊥,⊥) polarization.

We plot, in the top half of Fig. 4, the phonon frequency as a function of uniaxial stress along the [001] direction for pure (open circles and triangles) and heavily doped Si (filled circles and tri-

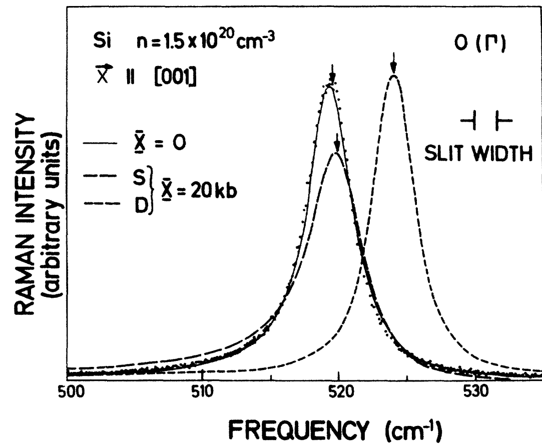

FIG. 3. Line shape of the optical phonon in heavily doped n-Si as a function of uniaxial stress along the [001] direction. The dots are experimental data at zero stress and the solid line a fit using Eq. (18a). The amplitude q, $\Gamma+\gamma$, and $\omega_0+\Delta\omega_0$ are adjusted for the best fit. The short dashes indicate the fit obtained for the doublet and the long dashes for the singlet at 20 kbar. Experimental data at 20 kbar are excluded for the sake of clarity. Note the decrease in asymmetry for the doublet and the increase for the singlet at 20 kbar. The relative intensities of the three peaks are accurate to within 10%. The arrows above the peaks indicate the phonon frequency used to fit the line shape (not coincident with the peak frequency for asymmetric line shapes).

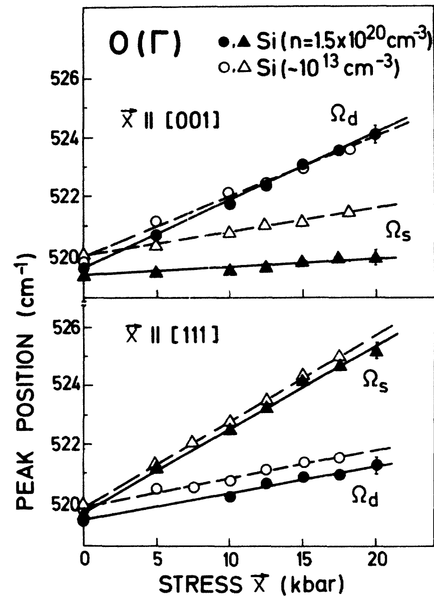

FIG. 4. Frequency of the optical phonon under uniaxial stress along the [001] and [111] directions for pure (open circles and triangles) and heavily doped (filled circles and triangles) Si. The circles and triangles denote the phonon doublet (Ω_d) and singlet (Ω_s), respectively.

TABLE II. Coefficients describing the splitting of the zone-center optical phonon under uniaxial stress in pure Si (units of 10^{28} sec^{-2}). The coefficients are defined in Appendix B.

Coefficient	Present measurements	Previous measurements
$p+2q$	-5.20 ± 0.26 [a]	-4.7 [a,b]
	-5.33 ± 0.26 [c]	-5.9 [b,c]
		-5.64 ± 0.33 [d]
p	-1.43 ± 0.07 [a]	-1.2 [a,b]
q	-1.89 ± 0.09 [a]	-1.8 [a,b]
r	-0.59 ± 0.03 [c]	-0.63 [b,c]

[a] [001] stress.
[b] Reference 21, uniaxial stress.
[c] [111] stress.
[d] Reference 22, hydrostatic stress.

angles). The circles and triangles represent the phonon doublet and singlet, respectively. At zero stress the frequency shift of the heavily doped Si with respect to the pure Si is -0.5 ± 0.2 cm^{-1}. This difference is observed to decrease for the doublet Ω_d as a high stress is reached, so that the frequency of the doublet in heavily doped Si reaches that of the doublet in pure Si. For the carrier enhanced singlet in the heavily doped Si, the frequency shift from pure Si increases with stress to a value of -1.4 ± 0.2 cm^{-1} at kbar.

The data for pure Si shown in Fig. 4 was obtained under the same conditions as for heavily doped Si, and is in agreement with previous measurements,[21] which were limited to about 12 kbar. The present measurements have been extended to a stress of 18 kbar. The coefficients describing the splitting of the phonon p, q, and r (defined in Appendix B) obtained from our measurements are listed in Table II.

The theoretical calculations performed for $\Delta\omega_0$, q, and Γ at zero and high stress are summarized in Table III, and compared with the experimental results obtained for an exciting wavelength of 6471 Å. In performing the calculations, we have used a Fermi level of 0.11 eV at zero stress. At this Fermi level $\hbar\omega_{min}=0$ and $\hbar\omega_{max}=0.88$ eV were used to calculate $\Delta\omega_0$. For the calculations at high stress, if we assume that all the carriers are in the singlet valleys at 20 kbar, we obtain a Fermi level of 0.24 eV. This is, however, an overestimate, since the splitting between the doublet and singlet, calculated from known band-deformation potentials[23] and elastic compliance constants,[24] is 0.18 eV at 20 kbar. In order to have the nominal electron density with this valley splitting we must have a Fermi level of 0.22 eV in the singlet and therefore 0.04 eV in the doublet. This means that 22% of the original number of carriers are still in the doublet valleys. For the above values of E_F we obtain $\hbar\omega_{max}=1.06$ eV and $\hbar\omega_{min}=0.18$ eV for the singlet and $\hbar\omega_{max}=0.8$ eV and $\hbar\omega_{min}=0.18$ eV for the doublet. Using these values the parameters $\Delta\omega_0$, q, and Γ for the phonon singlet and doublet were calculated as described in Sec. III. As shown in Table III, the agreement between theory and experiment for $\Delta\omega_0$ is excellent. Good agreement is also found for the values of q for zero stress and the singlet. For the doublet, the q obtained from the fit to experiment was rather insensitive to the numerical value. Theoretically, it is actually only possible to say that q is very large because of the value of $\Gamma\simeq0$ (the electronic background barely overlaps with the phonon). The calculated broadening agrees only qualitatively with experiment. The broadening of pure Si, γ, taken to be 1.55 ± 0.1 cm^{-1} was subtracted from the experimental linewidth to give Γ (Table III, Ref. a). One observes, however, that even though q is quite high for the doublet and both q and $\Gamma+\gamma$ do not change appreciably between 12 and 20 kbar, suggesting a sufficient decoupling of the valleys, the experimental broadening does not reach that of pure Si. This suggests, as already mentioned, that there may be other contributions, such as disorder or the effect of atomic masses of the dopant in these heavily doped crystals, that contributes to broadening. If we took the broadening of the doublet to be the "intrinsic" broadening and subtracted that to obtain the linewidth due to the Fano interaction (Table III, Ref. b), we get a more reasonable agreement with the theoretical calculations. In view of the rather large errors in the measurements of Γ, we believe that q and

TABLE III. Experimental and calculated values of q, Γ, and $\Delta\omega_0$ at zero and high stress (20 kbar) along the [001] direction for n-Si ($n=1.5\times10^{-20}$ cm^{-3}). Exciting wavelength = 6471 Å.

		q	Γ (cm^{-1})	$\Delta\omega_0$ (cm^{-1})
Zero stress	Expt.	-24 ± 2	0.32 ± 0.14 [a]	-0.5 ± 0.2
			0.11 ± 0.14 [b]	
	Theor.	-21^{+8}_{-4}	0.14 ± 0.04	-0.65
20-kbar doublet	Expt.	-100^{+50}_{-20}	0.21 ± 0.14 [a]	0 ± 0.2
			0 ± 0.14 [b]	
	Theor.	high	0	-0.10
20-kbar singlet	Expt.	-9 ± 1	0.75 ± 0.14 [a]	-1.4 ± 0.2
			0.54 ± 0.14 [b]	
	Theor.	-12 [c]	0.31	-1.50 [c]

[a] Γ obtained by subtracting γ(pure Si) = 1.55 ± 0.1 cm^{-1}.
[b] Γ obtained by subtracting γ(doublet, 20 kb) = 1.76 ± 0.14 cm^{-1}.
[c] The contribution from the filled part $\Delta'\omega_0$ is included in these values.

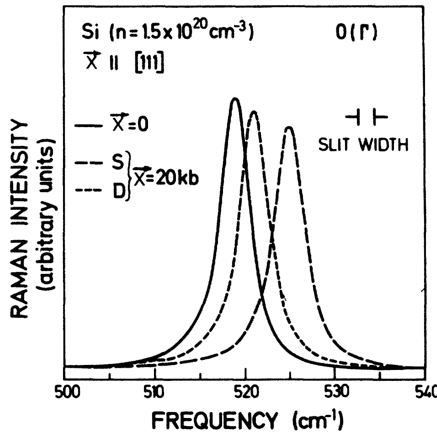

FIG. 5. Line shape of the optical phonon in heavily doped n-Si as a function of uniaxial stress along the [111] direction. The solid line is the curve for zero stress, the short- and long-dashed lines for the doublet and singlet, respectively, at 20 kbar. The line shapes of the peaks do not change with stress. The intensity of the doublet is on a 4× expanded scale after correcting for grating efficiency.

$\Delta\omega_0$ are better indicators of the success of the theory than Γ.

The application of a [111] uniaxial stress leaves all the conduction band valleys equivalent. The valley populations remain unchanged, therefore the parameters q, Γ, and $\Delta\omega_0$ should not change for either phonon singlet or doublet when a stress is applied. That $\Delta\omega_0$ remains unchanged is demonstrated in the lower half of Fig. 4, where we plot the phonon frequencies as a function of [111] stress for pure and heavily doped Si. The zero-frequency shift between them is maintained for the singlet and doublet as a function of stress. The phonon line shapes for [111] stress are plotted in Fig. 5. The asymmetry and broadening remain unchanged up to 20 kbar within experimental error.

While this result may sound reasonable, we should point out that all X_1 points are expected to split under a [111] stress. This splitting has been calculated[13] to be ≃100 meV at 20 kbar, a splitting that within our model should lead to some change in Γ and $\Delta\omega_0$. We have neither observed this change nor the associated change in q. We cannot offer, at this point, any plausible explanation of this observation.

C. Second-order acoustical phonon 2TA(X)

We have also measured the frequency of the second-order acoustical phonon 2TA(X) as a function of uniaxial stress along the [001] and [111] directions for both pure and heavily doped n-Si. A clear spectrum whose shift could be easily measured was obtained with 400 mW of 5145-Å radiation. The shift in the frequency of this phonon of mainly Γ_1 symmetry is expected to be only due to the hydrostatic component of the stress. The experimental results indicate that this is indeed true. In Fig. 6 we plot the frequency of the phonon as a function of applied uniaxial stress along the [001] and [111] directions. There is a linear shift to lower frequency. No change in line shape was observed. The slope $\partial\omega_1/\partial F$, where F is the hydrostatic stress ($F=\frac{1}{3}X$ in our case), is the same within experimental error for both stress directions and for both pure and heavily doped n-Si. In Table IV we list the mode Grüneisen parameters γ_1 obtained by our measurements. γ_1 is defined as

$$\gamma_1=\frac{1}{\chi_T\omega_1}\frac{\partial\omega_1}{\partial F}\ , \tag{21}$$

where χ_T is the isothermal compressibility, taken to be[15] 1.012×10^{-12} cm^2/dyn, and ω_1 is the frequency of the 2TA(X) phonon. Our measurements confirm both the sign and magnitude obtained by earlier work.

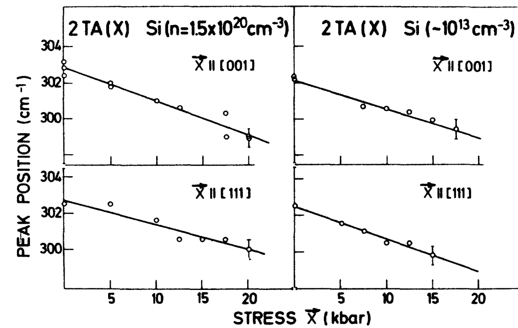

FIG. 6. Frequency of the second-order acoustical phonon 2TA(X) as a function of applied uniaxial stress along the [001] and [111] directions for pure and heavily dopes n-Si. The circles are experimental points and the solid lines are linear least-squares fits.

TABLE IV. The mode Grüneisen parameter γ_1 for 2TA(X) scattering for pure and heavily doped n-Si.

Material	Present work	Previous work
Pure Si	-1.52 ± 0.3 [a]	-1.4 ± 0.2 [b]
(~10^{13} cm^{-3})	-1.75 ± 0.3 [c]	-1.4 ± 0.3 [d]
		-1.74 ± 0.21 [e]
Heavily doped	-1.81 ± 0.3 [a]	
n-Si	-1.35 ± 0.3 [c]	
($n=1.5\times10^{20}$ cm^{-3})		

[a] [001] stress.
[b] Reference 25, hydrostatic stress, Raman scattering.
[c] [111] stress.
[d] Reference 22, hydrostatic stress, Raman scattering.
[e] Reference 26, uniaxial stress, neutron scattering.

V. CONCLUSIONS

We have investigated the effects of interband transitions on the phonon spectra in heavily doped n-Si. The zone-center optical phonon exhibits a Fano-type line shape due to the discrete-continuum interaction, while there is no effect on the second-order acoustical spectrum. We studied the Fano-type line shapes in detail, as a function of exciting frequency and uniaxial stress. The parameters that describe the Fano interaction—the asymmetry parameter q, the broadening Γ, and the frequency shift due to the self-energy $\Delta\omega_0$—were calculated from microscopic theory. A purely algebraic approach, assuming parabolic conduction bands, is used to obtain theoretical values of the three parameters that are in excellent agreement with experiment. The results confirm the sign and magnitude of the deformation potential D_0 for the coupling of the Δ_1-$\Delta_{2'}$ conduction bands by the optical phonon ($D_0 = -8.08$ eV) obtained from pseudopotential theory.

The second-order acoustical phonon 2TA(X) was studied under uniaxial stress for both pure and heavily doped n-Si. The shift in the frequency con firms the sign and magnitude of this shift obtained previously by hydrostatic pressure measurements, and is the same within experimental error for both pure and heavily doped Si.

APPENDIX A

In order to determine q [Eq. (1c)], the signs of V and T_e should be determined in a consistent manner, using the same set of valence- and conduction-band wave functions. The signs of the other three parameters that enter into the calculation of q are known: Γ (positive), $\Delta\omega_0$ (negative, as found in Sec. IV A), and T_p (negative, Ref. 20).

The wave functions of the conduction bands at the X_1 point along the [001] direction can be written as linear combinations of the basis[27]

$$u_1 = \frac{[110] - [\bar{1}\bar{1}0]}{\sqrt{2}}, \quad u_3 = \frac{[1\bar{1}0] + [\bar{1}10]}{\sqrt{2}},$$
$$u_2 = \frac{[001] - [00\bar{1}]}{\sqrt{2}}, \quad u_4 = \frac{[001] + [00\bar{1}]}{\sqrt{2}}, \tag{A1}$$

where

$$[hkl] = \exp[i(2\pi/a)(hx + ky + lz)]. \tag{A2}$$

The wave functions obtained by finding the eigenvectors of Eq. (34) in Ref. 27 are

$$2^{-1/2}[\beta(u_1 + u_3) + \alpha(u_2 + u_4)] \quad \text{for } \Delta_1$$

and (A3)

$$2^{-1/2}[\beta(u_3 - u_1) + \alpha(u_4 - u_2)] \quad \text{for } \Delta_{2'} .$$

With the pseudopotential coefficients[28] $v_3 = -0.21$ Ry and $v_8 = 0.04$ Ry we find $\beta = 0.89$, $\alpha = -0.46$.

The electron-phonon interaction potential V_{ep} is expanded in terms of plane waves

$$V_{ep} = \sum_G v_G \cos(\vec{G} \cdot \vec{L}) e^{i\vec{G} \cdot \vec{r}}. \tag{A4}$$

The summation runs over all reciprocal-lattice vectors $\vec{G}$. $e^{i\vec{G}\cdot\vec{r}}$ is the plane wave corresponding to $\vec{G}$ and v_G is the pseudopotential coefficient written in the standard form $v_{b^2+c^2+d^2}$ for a reciprocal-lattice vector $\vec{G} \equiv (b, c, d)$. $\vec{L}$ is the position vector, $\frac{1}{8}a(1,1,1+\delta)$, corresponding to an atom at $\frac{1}{8}a(1,1,1)$ displaced by a [001] phonon by $a\delta/8$. Upon expanding V_{ep} the only components that have nonzero matrix elements between the Δ_1 and $\Delta_{2'}$ conduction bands are those corresponding to the reciprocal-lattice vectors $\langle 111 \rangle$ and $\langle 200 \rangle$, which are, respectively

$$V_{ep,3} = -v_3(\delta\pi/4\sqrt{2})([111] + [1\bar{1}\bar{1}] + [\bar{1}1\bar{1}]$$
$$- [\bar{1}\bar{1}1] + [\bar{1}\bar{1}\bar{1}] + [\bar{1}11] + [1\bar{1}1] - [11\bar{1}]),$$
$$V_{ep,4} = -v_4(\pi\delta/2)([002] + [00\bar{2}]) . \tag{A5}$$

The matrix element for the electron-phonon interaction between the Δ_1 and $\Delta_{2'}$ bands is

$$\langle \Delta_1 | V_{ep,3} + V_{ep,4} | \Delta_{2'} \rangle = -\tfrac{1}{2}\pi\delta(\sqrt{2}\,\beta\alpha v_3 + \alpha^2 v_4) . \tag{A6}$$

We have defined the electron-phonon matrix element V in terms of the deformation potential D_0 [Eq. (9)] such that D_0 is the interaction for one atom moving $\frac{1}{2}a$. If we set $\frac{1}{8}a\delta = \frac{1}{2}a$, i.e., $\delta = 4$, we obtain from Eq. (A6),

$$D_0 = -2\pi(\sqrt{2}\,\beta\alpha v_3 + \alpha^2 v_4) . \tag{A7}$$

Substituting the values of the pseudopotential coefficients from Ref. 28 ($v_3 = -0.21$ Ry, $v_4 = -0.13$ Ry), we obtain

$$D_0 = -8.08 \text{ eV}. \tag{A8}$$

Other factors in the expression for V [Eq. (9)] being positive, the sign of V is negative.

The electronic matrix element T_e is calculated using Eqs. (A3) and the wave functions of the X_4 valence band[27]

$$u_5 = \frac{[110] + [\bar{1}\bar{1}0]}{\sqrt{2}}, \quad u_6 = \frac{[1\bar{1}0] - [\bar{1}10]}{\sqrt{2}} . \tag{A9}$$

The transition matrix elements are

$$\langle \Delta_{2'} | p_x | u_5 \rangle \langle u_5 | p_y | \Delta_1 \rangle = \langle \Delta_{2'} | p_x | u_6 \rangle \langle u_6 | p_y | \Delta_1 \rangle$$
$$= -\tfrac{1}{2}(2\pi/a)^2 \hbar^2 \beta^2 . \tag{A10}$$

The expression for T_e [Eq. (17)] becomes

$$T_e = -(2e^2/m^2)(2\pi/a)^2\hbar^2\beta^2 \times\{[\hbar\Omega-(E_v-E_c)]^{-1}-[\hbar\Omega+(E_v-E_c)]^{-1}\}\ , \quad \text{(A11)}$$

which is negative for $\hbar\Omega$ below the E_2 gap, $E_c - E_v = 4.4$ eV.

APPENDIX B

For a uniaxial stress applied along either the [001] or [111] directions, the threefold degeneracy of the zone-center optical phonon is lifted. The phonon splits into a singlet Ω_s and a doublet Ω_d. There is also a shift in the frequency of the phonon $\Delta\Omega_h$, due to the hydrostatic component of the stress. The frequencies of the singlet and doublet, respectively, are given by[21]

$$\begin{aligned}\Omega_s &= \omega_0 + \Delta\Omega_h + \tfrac{2}{3}\Delta\Omega\ ,\\ \Omega_d &= \omega_0 + \Delta\Omega_h - \tfrac{1}{3}\Delta\Omega\ .\end{aligned} \quad \text{(B1)}$$

The hydrostatic shift is given by

$$\Delta\Omega_h = (X/6\omega_0)(p+2q)(S_{11}+2S_{12})\ , \quad \text{(B2)}$$

while the singlet-doublet splitting is

$$\Delta\Omega = \begin{cases}\dfrac{X}{2\omega_0}(p-q)(S_{11}-S_{12}) & \text{for } \vec{X}\parallel[001]\ ,\\[2ex] \dfrac{X}{2\omega_0}\, rS_{44} & \text{for } \vec{X}\parallel[111]\ ,\end{cases} \quad \text{(B3)}$$

where S_{11}, S_{12}, and S_{44} are the elastic compliance constants.[24] The constants p, q, and r, intrinsic to the material, are therefore completely determined by the application of uniaxial stresses along the [001] and [111] directions.

---

*Formerly Meera Chandrapal.

†On leave from the University of Toulouse, France.

[1]M. Jouanne, R. Beserman, I. Ipatova, and A. Subashiev, Solid State Commun. 16, 1047 (1975).

[2]M. Chandrasekhar, J. B. Renucci, M. Cardona, and E. O. Kane, *Proceedings of the Thirteenth International Conference on the Physics of Semiconductors, Rome, 1976,* edited by F. G. Fumi (Tipografia Marves, Rome, 1977), p. 255; M. Chandrasekhar, M. Cardona, and E. O. Kane, Phys. Rev. B 16, 3579 (1977).

[3]U. Fano, Phys. Rev. 124, 1866 (1961).

[4]F. Cerdeira, T. A. Fjeldly, and M. Cardona, Phys. Rev. B 8, 4734 (1973).

[5]M. Chandrasekhar and M. Cardona, *Proceedings of the Third International Conference on Lattice Dynamics, Paris,* 1977, edited by M. Balkanski (Flammarion, Paris, 1978).

[6]I. P. Ipatova and A. V. Subashiev, in Ref. 2, p. 279.

[7]J. B. Renucci, R. N. Tyte, and M. Cardona, Phys. Rev. B 11, 3885 (1975).

[8]R. Zeyher, H. Bilz, and M. Cardona, Solid State Commun. 19, 57 (1976).

[9]H. Vogelmann and T. A. Fjeldly, Rev. Sci. Instrum. 45, 309 (1974).

[10]Obtained from Monsanto Chemical Co.

[11]M. V. Klein, *Light Scattering in Solids*, edited by M. Cardona (Springer-Verlag, New York, 1975).

[12]M. Cardona and F. H. Pollak, Phys. Rev. 142, 530 (1966).

[13]P. Melz, J. Phys. Chem. Solids 32, 209 (1971).

[14]J. C. Hensel, H. Hasegawa, and M. Nakayama, Phys. Rev. 138, A225 (1965).

[15]For example, C. Kittel, *Introduction to Solid State Physics* (Wiley, New York, 1971), p. 249.

[16]F. Cerdeira, Ph.D. thesis (Brown University, Providence, R.I., 1972) (unpublished).

[17]F. Cerdeira and M. Cardona, Phys. Rev. B 5, 1440 (1972). Owing to an algebraic error in this paper and in Ref. 16, the magnitude of $D_0(\mathcal{E}^*_{20})$ is not 2.02 eV as quoted, but 8 eV.

[18]V. I. Fistul', *Heavily Doped Semiconductors* (Plenum, New York, 1969), p. 63.

[19]L. R. Swanson and A. A. Maradudin, Solid State Commun. 8, 859 (1970).

[20]M. Cardona, F. Cerdeira, and T. A. Fjeldly, Phys. Rev. B 10, 3433 (1974).

[21]E. Anastassakis, A. Pinczuk, E. Burstein, F. H. Pollak, and M. Cardona, Solid State Commun. 8, 133 (1970).

[22]B. A. Weinstein and G. J. Piermarini, Phys. Rev. B 12, 1172 (1975).

[23]V. J. Tekippe, H. R. Chandrasekhar, P. Fisher, and A. K. Ramdas, Phys. Rev. B 6, 2348 (1972), and references therein.

[24]J. J. Hall, Phys. Rev. 161, 756 (1967).

[25]W. Richter, J. B. Renucci, and M. Cardona, Solid State Commun. 16, 131 (1975).

[26]J. Prechtel, E. Lüscher, and J. Kalus, J. Phys. E 10, 432 (1977); and J. Prechtel, Ph.D. thesis (Technische Universität München, 1976) (unpublished).

[27]M. Cardona, *Atomic Structure and Properties of Solids* (Academic, New York, 1972), p. 514.

[28]D. Brust, Phys. Rev. A 134, 1337 (1964). v_4, as quoted in Ref. 16, was obtained by interpolating the values in this article using the curves in A. O. E. Animalu and V. Heine, Philos. Mag. 12, 1249 (1965).